Journal of the Serbian Chemical Society
JSCS-info@shd.org.rs • www.shd.org.rs/JSCS
J. Serb. Chem. Soc. *90* (7–8) 929–942 (2025)
JSCS–5430
Original scientific paper
Published 17 August, 2025

Innovation in printer ink based on carbon quantum dots (CQDs) derived from styrofoam waste for anti-counterfeiting document technology

MUHAMMAD FEBRIANSYAH[1], DEVINDA K. PUTRI[1], ANGGUN T. NABILA[1], ILHAM RADIANSYAH[2], MUHAMMAD NURRAHMAN[3] and I NYOMAN CANDRA[1]*

[1]*Chemistry Education Study Program, University of Bengkulu, Bengkulu, 38371, Indonesia,* [2]*Natural Science Education Study Program, University of Bengkulu, Bengkulu, 38371, Indonesia and* [3]*Department of Chemistry, University of Bengkulu, Bengkulu, 38371, Indonesia*

(Received 17 March, revised 26 March, accepted 26 May 2025)

Abstract: In response to the dual challenges of the environmental plastic pollution and the rise of document forgery, this study presents a novel fluorescent printer ink based on nitrogen and boron co-doped carbon quantum dots (N,B--codoped CQDs) derived from styrofoam waste. The CQDs were synthesized using a microwave-assisted green synthesis approach, and their photoluminescent properties were tailored *via* co-doping with urea and boric acid. The resulting ink formulation not only exhibited strong dual-colour fluorescence under 365 and 532 nm excitation but also demonstrated effective printability and stability on standard paper substrates. Characterization techniques, including UV––Vis spectrophotometry, fluorescence emission, Fourier-transform infrared spectroscopy and high-resolution transmission electron microscopy confirmed the successful incorporation of heteroatoms and the formation of nanoscale amorphous CQDs with rich surface functionality. Compared to the commercial printer ink, the N,B-codoped CQDs printer ink offered superior anti-counterfeiting features through fluorescence activation, albeit with a slightly lower ink absorption rate (0.47±0.14 *vs*. 0.74±0.06 cm/min). This study introduces a low--cost, eco-friendly and scalable strategy for producing smart ink with potential applications in secure printing and sustainable nanomaterial development.

Keywords: N,B-codoped CQDs printer ink; styrofoam; fluorescence.

INTRODUCTION

The document forgery is a criminal act involving the use of falsified documents.[1] Such forgery may include counterfeit signatures, falsified document content, or forged origins of the documents.[2] This issue represents a global problem,

* Corresponding author. E-mail: inyomancandra@unib.ac.id
https://doi.org/10.2298/JSC250317038F

resulting in significant financial losses and posing security threats to individuals, companies, governments and society at large.[3] The Supreme Court of Indonesia recorded 37,757 cases of document forgery between 2021 and 2023.[4] Consequently, the need for anti-counterfeiting technology has become increasingly crucial to protect documents against increasingly sophisticated forgery attempts.

In parallel with this security concern, the issue of environmental sustainability – particularly plastic waste pollution – has also become a pressing global challenge. One major contributor to this problem is the increasing use of styrofoam as food packaging, driven by the rising demand for online food purchases, especially among street vendors and small-scale traders. This popularity stems from styrofoam's affordability, light weight, water resistance, practicality and accessibility. However, despite its practical advantages, styrofoam poses significant environmental threats because it is a non-degradable plastic that often accumulates in landfills or pollutes oceans.[5] Styrofoam is a significant contributor to environmental pollution and is categorized as the fifth largest waste material globally.[6,7]

Interestingly, the recent advances in nanotechnology have revealed that this problematic waste material can be transformed into high-value nanomaterials. Styrofoam, made from polystyrene polymer, contains styrene monomers that can be used to synthesize carbon quantum dots (CQDs). Several studies have successfully synthesized carbon-based quantum dots from styrofoam waste.[8] This approach does not only reduces environmental pollution but also creates value by enabling the development of eco-friendly fluorescent inks for anti-counterfeiting applications. CQDs are particularly well-suited for such applications due to their low toxicity, ease of synthesis, and cost-effectiveness.[9] Furthermore, styrofoam's high carbon content (approximately 62.6–92.2 %) and its low cost make it an ideal precursor for sustainable CQDs synthesis.[10]

To understand their application potential, it is essential to examine the fundamental characteristics of CQDs. These nanomaterials, typically smaller than 10 nm, are composed of fluorescent graphite-like cores.[11,12] Their fluorescence originates from π-conjugated bandgap transitions and surface defect states.[13,14] However, undoped CQDs generally exhibit low fluorescence quantum yields (*FQY*), around 10 %.[15] Doping with heteroatoms such as nitrogen can significantly enhance their *FQY*, reaching up to 49 %.[16] Co-doping strategies – such as combining nitrogen from ethylenediamine and boron from boric acid – have achieved *FQY* values around 39 %. In addition, sulphur and oxygen co-doping has been shown to enable dual-color emission (blue and red).[15] Eda *et al.*[17] reported that nitrogen and boron co-doped carbon quantum dots (N,B-codoped CQDs) emit distinct blue and yellow fluorescence, respectively. These findings underscore the tunable optical properties of heteroatom-doped CQDs, which are particularly valuable in multi-color anti-counterfeiting technologies.

The recent studies have increasingly explored the use of CQDs for anti-counterfeiting applications, focusing on their tunable fluorescence and low toxicity. For example, Deng *et al.*[9] synthesized CQDs *via* a solvothermal method using ascorbic acid as a carbon source, but his work did not explore the use of eco-friendly waste materials or their scalability in industrial printing. Similarly, Eskalen *et al.*[18] successfully derived blue-fluorescent CQDs from *Laurus nobilis* leaves, yet his study lacked an evaluation of ink absorption behaviour. Eda *et al.*[17] research demonstrated promising dual-color emission from N,B-codoped CQDs but did not assess printing performance, particularly the crucial parameter of ink absorption rate.

This study seeks to bridge these gaps by synthesizing N,B-codoped CQDs from styrofoam waste and formulating them into printer ink. It focuses not only on the sustainable and low-cost production of fluorescent N,B-codoped CQDs but also on evaluating their performance in anti-counterfeiting document printing, specifically regarding ink absorption efficiency.

EXPERIMENTAL

Materials

Locally collected styrofoam waste (Bengkulu, Indonesia) was used as the primary carbon source. Monohydrate citric acid ($C_6H_8O_7 \cdot H_2O$, 210.14 g mol^{-1}), boric acid (H_3BO_3, 61.83 g mol^{-1}), and urea ($(NH_2)_2CO$, 60.06 g mol^{-1}), all analytical grade, served as dopant precursors. These chemicals were procured from Emsure® Merck and used without further purification. Activated charcoal and technical grade ethanol (96 %) were used, with ethanol serving as the solvent.

Preparation of styrofoam waste

Styrofoam waste was washed thoroughly under running water to remove surface impurities and air-dried. The dried styrofoam was chopped into small pieces and heated in an oven at 240 °C for varying durations of 30, 60, 90, 120 and 150 min. After softening, the material was ground into fine powder using a laboratory grinder and sieved through a 100-mesh sieve to ensure uniform particle size. The resulting powder was stored in an airtight container for subsequent use.

Synthesis of N,B-codoped CQDs

N,B-codoped CQDs were synthesised *via* microwave-assisted synthesis based on the method reported by Alkian *et al.*[19] with slight modifications in precursor ratios and microwave exposure time. 1 g of styrofoam powder was mixed with 1 g each of citric acid, boric acid and urea in a 250 mL glass beaker. To facilitate homogenisation, 2 mL of distilled water was added to the mixture, which was then heated in a microwave oven for 5 min. After cooling, 25 mL of 96 % ethanol was added, and the mixture was stirred thoroughly. The solution was filtered using standard filter paper to separate the filtrate containing the N,B-codoped CQDs from the solid residue. UV irradiation (365 nm) of the filtrate produced a cyan-blue emission, while irradiation with a green laser (532 nm) yielded yellow fluorescence, confirming successful N,B-codoped CQDs formation.

Characterization of N,B-codoped CQDs

The optical properties of the synthesised CQDs were analysed using a Thermo Scientific Genesys 50 UV–Vis spectrophotometer in the wavelength range of 250–800 nm. Fluorescence

characteristics were assessed using a Horiba FluoroMax hybrid fluorescence spectroscopy steady state and life time system. All samples for UV–Vis and fluorescence measurements were prepared using identical dilution volumes, without quantitative concentration calibration. Functional group analysis was conducted using a Bruker Alpha II FTIR spectrometer. The particle morphology, interplanar spacing, and selected area electron diffraction (SAED) patterns were investigated using a high-resolution transmission electron microscope (HRTEM) Talos F200X.

Preparation of N,B-codoped CQDs-based printer ink

The printer ink formulation was adapted from the method reported by Sari *et al.*[20] with adjustments made to the concentrations of activated charcoal and the gum arabic-to-water ratio to improve stability and fluorescence. A 10 mL portion of the N,B-codoped CQDs solution was mixed with 2 g of activated charcoal under constant stirring. Separately, 3.5 g of gum arabic was dissolved in 20 mL of distilled water. The two solutions were combined and homogenised. UV irradiation at 365 nm confirmed the successful formulation through the observation of blue fluorescence.

Testing of N,B-codoped CQDs-based printer ink

The ink absorption rate was evaluated using a capillary rise method adapted from previous studies.[20] A strip of standard A4 printing paper was cut to dimensions of 2 cm×15 cm and vertically immersed to a depth of 1 cm into each ink formulation for precisely 2 min. Immediately upon removal, the total length of ink rise (*i.e.*, the distance from the base of the strip to the furthest visible color front) was measured in cm using a ruler. This experiment was repeated five times for each ink type to ensure reproducibility.

The absorption rate (cm/min) was calculated using the formula:[20]

$$\text{Absorption rate} = \text{Absorption length}/\text{Immersion time} \quad (1)$$

For the printing test, the printer ink was loaded into an empty Canon iP2700 ink cartridge. The printed outputs were then exposed to UV light at 365 nm to observe fluorescence, confirming the presence and activity of the N,B-codoped CQDs within the printed material.

RESULTS AND DISCUSSION

Qualitative evaluation of N,B-codoped CQDs using laser illumination

The successful synthesis of N,B-codoped CQDs is visually confirmed under various lighting conditions, as illustrated in Fig. 1.

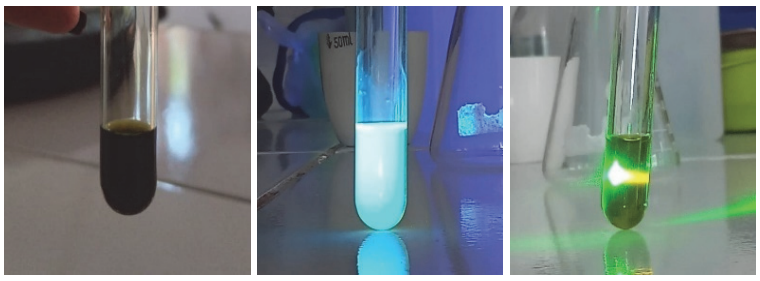

(a) (b) (c)

Fig. 1. Visual appearance of N,B-codoped CQDs solution under: a) normal lighting, b) UV laser (365 nm) and c) green laser (532 nm).

Under ambient lighting (Fig. 1a), the N,B-codoped CQDs solution exhibits a dark green color. Upon excitation with a 365 nm UV laser (Fig. 1b), it emits a strong cyan-blue fluorescence, which is attributed to the surface defect states and functional groups that facilitate radiative recombination of photoexcited electron–hole pairs. This phenomenon is consistent with prior studies highlighting the pivotal role of surface chemistry in determining carbon dot emission behaviour, particularly the involvement of sp^2 domains and defect-related energy states in generating blue-shifted luminescence.[21] Upon the exposure to a 532 nm green laser (Fig. 1c), the solution displays a yellow emission, suggesting longer-wavelength transitions associated with deeper surface states or boron-induced mid-gap trap levels. This excitation-dependent, multicolor emission behaviour underscores the tunable photoluminescence of the N,B-codoped system, in line with observations by Feng *et al.*[22] who emphasized the role of heteroatom doping in modulating the emissive characteristics of CQDs.

Morphological and structural analysis via HRTEM

Fig. 2. presents the morphology, crystallinity and size distribution of the synthesized N,B-codoped CQDs.

The HRTEM images in Fig. 2a and b reveal the quasi-spherical morphology and uniform dispersion of the N,B-codoped CQDs. A magnified HRTEM image (Fig. 2c) displays a clear dark-light fringe pattern with an interplanar spacing of 0.28 nm. This dark-light pattern signifies the presence of sp^2 hybridization in the core carbon atoms, further supporting the structural integrity of the N,B-codoped CQDs.[23] This spacing is comparable to those reported by Eda *et al.*[17] (0.25 nm) and Qu *et al.*[23] (~0.21 nm), suggesting partial graphitization of the carbon core.[23]

The SAED pattern (Fig. 2d) exhibits the diffuse diffraction rings characteristic of amorphous carbon, consistent with synthesis conducted at 240 °C. This observation agrees with the findings of Yadav *et al.*[14] who reported that synthesis temperatures below 300 °C favour amorphous carbon formation, whereas higher temperatures promote the development of graphitic crystallites. The particle size distribution (Fig. 2e) reveals an average diameter of 5.7 nm, which falls within the typical size range for CQDs (<10 nm).[14] Collectively, the HRTEM analysis confirm the successful synthesis of amorphous N,B-codoped CQDs with the desired structural features, interplanar spacing, and nanoscale size distribution.

Optical properties via *UV–Vis spectrophotometry*

The UV–Vis absorbance spectra of the N,B-codoped CQDs at varying synthesis times are shown in Fig. 3.

The UV–Vis spectrum of the N,B-codoped CQDs displays a prominent absorption peak at 348 nm, attributed to the n–π* transition of the C=O bond. This electronic transition typically occurs within the 300–500 nm range and aligns with

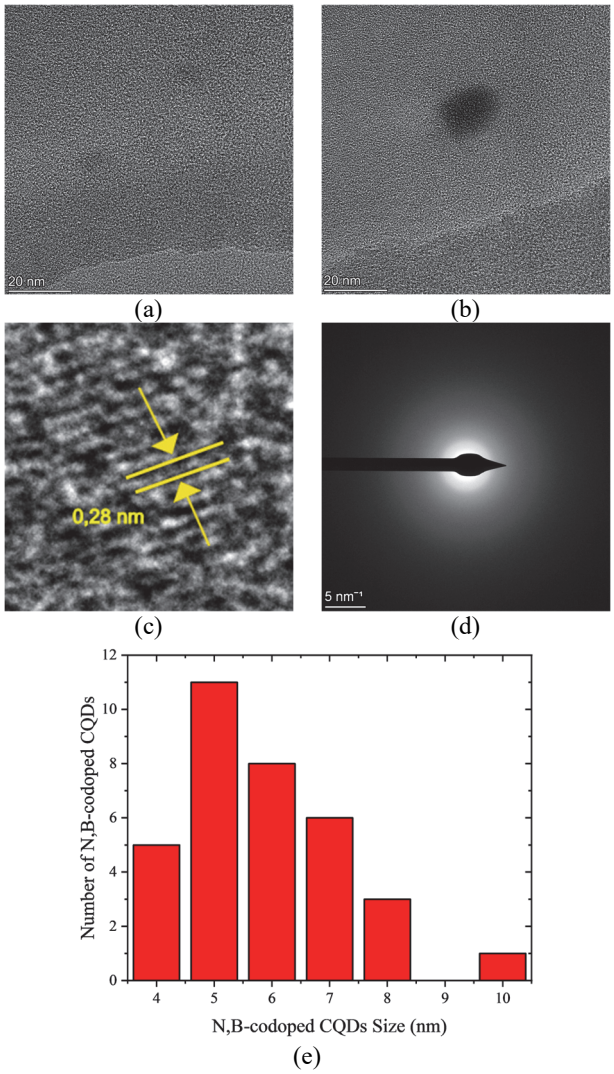

Fig. 2. A and b) HRTEM images of N,B-codoped CQDs; c) magnified HRTEM image showing interplanar spacing; d) SAED pattern of N,B-codoped CQDs; e) particle size distribution.

previous findings by Yuniarti *et al.*[24] and Kasmiarno *et al.*[25] In addition, a π–π* transition associated with C=C bonds is observed between 250–300 nm range.[25,26] These features reflect the intrinsic optical characteristics of N,B-codoped CQDs, which are influenced by both surface functional groups and the core structure.[27]

The synthesis duration plays a critical role in tuning the surface chemistry and, consequently, the optical absorption behaviour of the CQDs.[14,25] As illustrated in Fig. 3, the optimal synthesis time is identified at 90 min. At shorter durations, the

N,B-codoped CQDs exhibit insufficient surface development, resulting in reduced absorbance intensity. In contrast, N,B-codoped CQDs synthesised for 90 min demonstrate enhanced structural homogeneity and a higher density of functional groups, particularly those contributing to n–π* transitions, thereby yielding a more pronounced absorption peak.[25,26] Beyond this optimal synthesis time, extended thermal treatment induces surface degradation, possibly due to the over-oxidation or the particle aggregation, leading to a decline in absorbance. These observations are consistent with the report by Kasmiarno *et al.*,[25] which highlights the adverse effects of prolonged synthesis on the structural and electronic integrity of CQDs. Hence, precise control of synthesis time is essential for optimizing the optical performance of N,B-codoped CQDs.

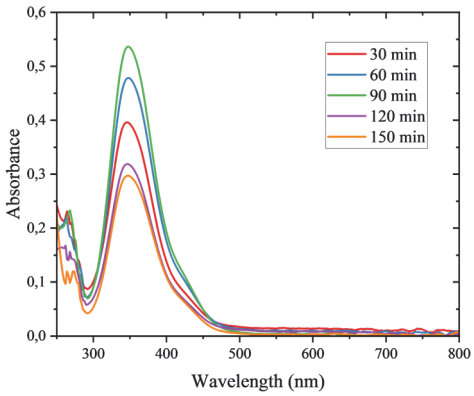

Fig. 3. UV–Vis absorbance spectra of N,B-codoped CQDs synthesized at different durations.

Photoluminescence analysis via *fluorescence spectroscopy*

The fluorescence spectra of the N,B-codoped CQDs are presented in Fig. 4.

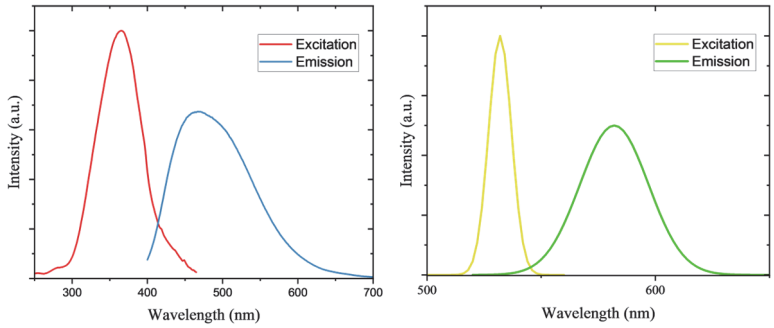

(a) (b)

Fig. 4. Fluorescence emission spectra of N,B-codoped CQDs: a) at 469 nm (λ_{ex} = 365 nm), b) at 582 nm (λ_{ex} = 532 nm).

Under 365 nm excitation, a prominent emission peak is observed at 469 nm, corresponding to the cyan-blue fluorescence, which is consistent with the visual observation under UV laser irradiation (Fig. 1b). In contrast, excitation at 532 nm results in an emission peak at 582 nm, yielding a yellow fluorescence, as visually demonstrated under green laser illumination (Fig. 1c). These emissions originate from the radiative recombination of photoexcited electron–hole pairs, facilitated by surface states and functional groups introduced through nitrogen and boron co--doping.[27,28] These dopant-related functional moieties play a significant role in enhancing the FQY and tuning the emission characteristics of the CQDs.[29–31] This finding is consistent with the study by Eda *et al.*[17] who reported a similar cyan--blue emission peak at 477 nm under 365 nm excitation, along with a secondary emission peak at 575 nm under 532 nm excitation, corresponding to yellow emission. Such dual-colour emission behaviour underscores the wavelength-dependent photoluminescent properties of N,B-codoped CQDs.

Functional group identification via *FTIR*

FTIR spectraof the N,B-codoped CQDs solution confirm, Fig. 5, the incurporation of nitrogen and boron functional groups.

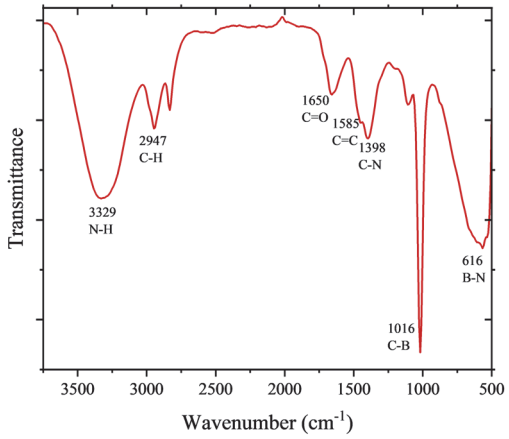

Fig. 5. FTIR spectrum of N,B-codoped CQDs.

The FTIR spectrum of the N,B-codoped CQDs solution exhibits the characteristic absorption peaks corresponding to various functional groups. The N–H stretching vibration appears at 3329 cm^{-1}, while the C–H stretching vibration is observed at 2947 cm^{-1}. Peaks at 1650 and 1585 cm^{-1} indicate the presence of C=C bonds and C=O stretching vibrations, respectively. Additional absorption bands at 1398, 1016 and 616 cm^{-1} correspond to C–N, C–B and B–N bonds, confirming the successful incorporation of nitrogen and boron during doping. The previous studies by Eda *et al.*[17] and Liu *et al.*[32] reported that the formation of N–H, C–N,

C–B and B–N bonds is characteristic of N,B-codoped CQDs, resulting from interactions between precursor materials and dopant atoms during synthesis. The presence of N–H and C–N groups suggests the effective nitrogen integration, which enhances the hydrophilicity and the surface reactivity of the CQDs. Similarly, the C–B and B–N functional groups confirm boron incorporation, playing a crucial role in modulating the electronic properties and surface chemistry.

These FTIR features further verify successful N and B doping, as evidenced by distinct absorption bands associated with these functional groups. The introduction of nitrogen and boron atoms is expected to generate some additional active sites, improving the optical performance of CQDs. Moreover, these functional groups contribute to the stabilization of surface states and influence the FQY of the nanomaterials.[15–17,29–31]

Qualitative comparison of N,B-codoped CQDs and commercial printer ink

The distinct fluorescent properties of N,B-codoped CQDs-based printer ink are compared with commercial printer ink in Fig. 6.

(a) (b)

Fig. 6. Comparison under: a) normal light and b) 365 nm UV laser between N,B-codoped CQDs and commercial printer ink.

Under normal lighting conditions, both the N,B-codoped CQDs ink and commercial printer ink appear black, exhibiting no discernible differences in visual appearance (Fig. 6a). However, upon exposure to a 365 nm UV laser, a marked contrast is observed: the N,B-codoped CQDs ink emits a bright cyan-blue fluorescence, whereas the commercial ink remains non-fluorescent (Fig. 6b). This cyan-blue emission directly stems from the inherent photoluminescent properties of the N,B-codoped CQDs,[17,33] confirming their successful incorporation into the ink formulation. The fluorescence observed in the N,B-codoped CQDs printer ink corresponds to the emission peak at 469 nm detected in the fluorescence spectrum of the CQDs solution (Fig. 4). In contrast, the absence of fluorescence in the commercial ink reflects the lack of N,B-codoped CQDs or analogous fluorescent components, further emphasizing the distinctive properties of the N,B-codoped CQDs printer ink.

Ink absorption rate comparison

Table I summarizes the ink absorption test comparing commercial and N,B--codoped CQDs printer ink formulations.

TABLE I. Comparison of absorption rate (cm/min) between commercial and N,B-codoped CQDs printer ink

Experiment no.	Material	
	Commercial printer ink	N,B-codoped CQDs printer ink
1	0.75	0.60
2	0.80	0.35
3	0.70	0.40
4	0.65	0.35
5	0.80	0.65
Mean ± *SD*, cm/min	0.74±0.065	0.47±0.144

The data presented in Table I reveal a notable difference in the absorption rates between commercial and N,B-codoped CQDs-based printer inks. The commercial ink exhibits a higher average absorption rate (0.74±0.065 cm/min) compared to the CQDs-based ink (0.47±0.144 cm/min). This discrepancy is primarily attributed to the compositional differences between the two formulations. Specifically, the absorption behaviour is influenced by the nature of the added compounds, particularly the surface-functionalised CQDs present in the latter.

Commercial printer inks typically contain organic dyes dispersed in solvent systems tailored to maximise penetration and drying efficiency on cellulose-based substrates.[34] These formulations often include the surfactants and humectants that enhance interaction with paper fibres, thereby increasing the absorption rate.[35] In contrast, the N,B-codoped CQDs-based ink incorporates these nanomaterials as its main functional component, significantly altering the ink's physicochemical profile. The structured and functionalised surfaces of the doped CQDs can reduce the mobility of the ink, thereby slowing its capillary-driven absorption into the paper matrix.

Furthermore, the presence of hydrophilic functional groups on the N,B-codoped CQDs surfaces modulates the interaction with the substrate, contributing to the observed lower absorption rate,[36] which because of slower absorption may initially be perceived as a drawback, it can actually enhance print quality by reducing ink feathering and improving colour uniformity. These characteristics make N,B-co-doped CQDs-based inks promising candidates for the high-resolution or the anti-counterfeiting printing applications, where precision and stability are essential.

Printing test of ink

Printed samples were tested under normal light and UV 365 nm in Fig. 7.

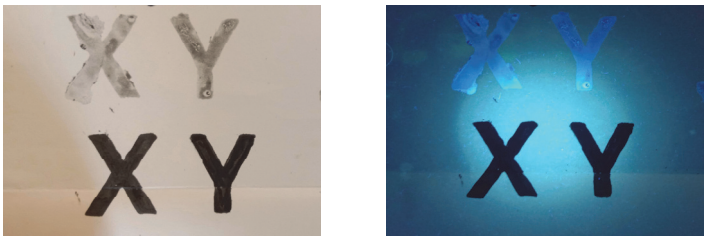

(a) (b)

Fig. 7. Printed paper samples using N,B-codoped CQDs-based printer ink (top) and commercial printer ink (bottom) under: (a) normal lighting, and (b) UV 365 nm illumination.

Fig. 7 compares the visual and fluorescent properties of printed paper using N,B-codoped CQDs and commercial printer ink. Under the normal lighting (Fig. 7a), the prints exhibit no discernible difference in appearance. However, upon exposure to the UV illumination at 365 nm (Fig. 7b), the N,B-codoped CQDs ink emits a distinct cyan-blue fluorescence, whereas the commercial printer ink shows no fluorescence. The observed cyan-blue emission arises from the photoluminescent characteristics of the N,B-codoped CQDs incorporated into the ink, which are attributed to their surface functional groups and the electronic transitions, consistent with the previous reports by Deng *et al.*[9] and Eskalen *et al.*[18] This fluorescence behavior corroborates the findings presented in Fig. 6, confirming the unique luminescent properties of the N,B-codoped CQDs printer ink under similar excitation.

The absence of fluorescence in the commercial ink highlights the enhanced functional capabilities of the N,B-codoped CQDs printer ink, which, unlike conventional inks relying solely on dyes or pigments,[35,36] incorporates nanomaterials that impart fluorescence and improved photostability. These properties present the N,B-codoped CQDs printer ink as particularly advantageous for applications in security printing, anti-counterfeiting and high-resolution imaging. Overall, the results validate the successful formulation of a fluorescent N,B-codoped CQDs--based printer ink.

CONCLUSION

This study successfully synthesized the N,B-codoped CQDs from styrofoam waste *via* a microwave-assisted method. The resulting N,B-codoped CQDs exhibited quasi-spherical morphology with an average size of 5.7 nm and an interplanar spacing of 0.28 nm, indicating partial graphitization. The fluorescence analysis revealed the emission peaks at 469 nm (λ_{ex} = 365 nm) and at 582 nm (λ_{ex} = 532 nm). FTIR confirmed the incorporation of N–H, C–N, C–B and B–N functional groups. The formulated N,B-codoped CQDs-based ink demonstrated strong cyan--blue fluorescence under UV light and effective printability on standard paper. Despite a lower average ink absorption rate (0.47±0.14 cm/min) compared to the commercial ink (0.74±0.06 cm/min), it provided superior anti-counterfeiting feat-

ures. In conclusion, the modified ink offers enhanced functionality and sustainability, making it a competitive and eco-friendly alternative to conventional commercial inks.

Acknowledgement. This research was funded by the Directorate of Learning and Student Affairs, Ministry of Education, Culture, Research, and Technology of the Republic of Indonesia through the Program Kreativitas Mahasiswa (PKM) Exact Sciences Research Scheme (Grant No. 2546/E2/DT.01.00/2024).

ИЗВОД

НОВИНА У ТОНЕРУ ЗА ШТАМПАЧ БАЗИРАНА НА УГЉЕНИЧНИМ КВАНТНИМ ТАЧКАМА (CQDs) ДОБИЈЕНИМ ИЗ ОТПАДА ОД СТИРОПОРА ЗА ТЕХНОЛОГИЈУ ПРОТИВ ФАЛИСИФИКОВАЊА ДОКУМЕНАТА

MUHAMMAD FEBRIANSYAH[1], DEVINDA K. PUTRI[1], ANGGUN T. NABILA[1], ILHAM RADIANSYAH[2], MUHAMMAD NURRAHMAN[3] и I NYOMAN CANDRA[1]

[1]Chemistry Education Study Program, University of Bengkulu, Bengkulu, 38371, Indonesia, [2]Natural Science Education Study Program, University of Bengkulu, Bengkulu, 38371, Indonesia u [3]Department of Chemistry, University of Bengkulu, Bengkulu, 38371, Indonesia

Као одговор на два проблема, загађење животне средина пластиком и пораст фалсификовања докумената, ова студија представља нови флуоресцентни тонер за штампач базиран на угљеничним квантним тачкама ко-допираним азотом и бором (N,B-кодопиране CQDs) синтетисаним из отпада од стиропора. CQDs су добијене приступом зелене синтезе подпомогнуте микроталасима, а њихове фотолуминесцентне особине су мењане ко-допирањем са уреом и борном киселином. Резултујућа формулација за тонер не само да је показала интензивну двобојну флуоресценцију под дејством побуђивачких таласних дужина од 365 и 532 nm, већ је показала и ефективну могућност штампања и стабилност на стандардним папирним супстратима. Техникама за карактеризацију које укључују UV–Vis спектрофотометрију, флуоресценту емисију, FTIR спектроскопију и трансмисиону електронску микроскопију високе резолуције (HRTEM), потврђена је успешна инкорпорација хетероатома и формирање аморфних на нанометарској скали CQDs са функционалном површином. У поређењу са комерцијалним тонером за штампач, тонер на бази N,B-кодопираних CQDs показује супериорне карактеристике за спречавање фалсификовања докумената кроз активацију флуоресценције, додуше уз нешто нижу брзину апсорпције тонера (0,47±0,14 наспрам 0,74±0,06 cm/min). Ова студија представља економичну, еколошки прихватљиву и прилагодљиву стратегију за производњу тонера са могућношћу примене у сигурном штампању и одрживом развоју наноматеријала.

(Примљено 17. марта, ревидирано 26. марта, прихваћено 26. маја 2025)

REFERENCES

1. D. Ormerod, K. Laird, M. Gibson, *Smith, Hogan, and Ormerod's criminal law*, Oxford University Press, Oxford, 2020 (https://doi.org/10.1093/he/9780198849704.001.0001)
2. A. Hadi, K. Anuar, H. Paino, *Manage. Accounting Rev. (MAR)* **15** (2016) 93 (https://ir.uitm.edu.my/id/eprint/30995)
3. Y. Liu, F. Han, F. Li, Y. Zhao, M. Chen, Z. Xu, X. Zheng, H. Hu, J. Yao, T. Guo, W. Lin, Y. Zheng, B. You, P. Liu, Y. Li, L. Qian, *Nature Commun*. **10** (2019) 2409 (https://doi.org/10.1038/s41467-019-10406-7)

4. Direktori Putusan Mahkamah Agung Republik Indonesia, https://putusan3.mahkamahagung.go.id/search.html?q=pemalsuan+dokumen&courtos=2 (accessed on January 4, 2024)
5. B. G. Kwon, K. Saido, L. Koizumi, H. Sato, N. Ogawa, S. Y. Chung, T. Kusui, Y. Kodera, K. Kogure, *Environ. Poll.* **188** (2014) 45 (https://doi.org/10.1016/j.envpol.2014.01.019)
6. E. Indarti, S. Muliani, S. Wulya, R. Rafiqah, I. Sulaiman, D. Yunita, *IOP Conf. Ser. Earth Env. Sci.* **711** (2021) 012011 (https://doi.org/10.1088/1755-1315/711/1/012011)
7. Annissa, P. E. Mathofani, S. Suriani, A. Sakinah, F. Polwandari, *KnE Soc. Sci.* **8** (2023) 53 (https://doi.org/10.18502/kss.v8i14.13816)
8. D. Kumar, S. Rani, B. Nanda, R. K. Srivastava, *ACS Sus. Chem. Eng.* **10** (2022) 1070 (https://doi.org/10.1021/acssuschemeng.1c08002)
9. Y. Deng, J. Qian, Y. Zhou, *ChemistrySelect* **5** (2020) 14930 (https://doi.org/10.1002/slct.202003487)
10. M. P. Aji, A. L. Wati, A. Priyanto, J. Karunawan, B. W. Nuryadin, E. Wibowo, P. Marwoto, N. Sulhadi, *Environ. Nanotech. Monit. Manage.* **9** (2018) 136 (https://doi.org/10.1016/j.enmm.2018.01.003)
11. K. J. Mintz, Y. Zhou, R. M. Leblanc, *Nanoscale* **11** (2019) 4634 (https://doi.org/10.1039/c8nr10059d)
12. J. Chen, J. Wei, P. Zhang, X. Niu, W. Zhao, Z. Zhu, H. Ding, H. Xiong, *ACS App. Mat. Interf.* **9** (2017) 18429 (https://doi.org/10.1021/acsami.7b03917)
13. M. J. Molaei, *RSC Adv*. **9** (2019) 6460 (https://doi.org/10.1039/c8ra08088g)
14. P. K. Yadav, S. Chandra, V. Kumar, D. Kumar, S. H. Hasan, *Catalysts* **13** (2023) 422 (https://doi.org/10.3390/catal13020422)
15. L. Li, L. Shi, J. Jia, O. Eltayeb, W. Lu, Y. Tang, C. Dong, S. Shuang, *ACS Appl. Mater. Interf.* **12** (2020) 18250 (https://doi.org/10.1021/acsami.0c00283)
16. N. T. N. Anh, A. D. Chowdhury, R. Doong, *Sens. Actuators, B* **252** (2017) 1169 (https://doi.org/10.1016/j.snb.2017.07.177)
17. S. J. Eda, M. Putriyani, N. O. Azhari, A. Bahtiar, *J. Ilmu Dan Inovasi Fisika* **8** (2024) 17 (https://doi.org/10.24198/jiif.v8i1.50454) (in Indonesian)
18. H. Eskalen, M. Kavgaci, A. Kayis, Ş. Özğan, *Eskişehir Tech. Univer. J. Sci. Technol., A* **22** (2021) 366 (https://doi.org/10.18038/estubtda.991595)
19. I. Alkian, A. Prasetio, L. Anggara, N. Karnaji, M. H. Fonisyah, Z. M. Rizka, H. Widiyandari, *J. Phys. Conf. Ser.* **1204** (2019) 012093 (https://doi.org/10.1088/1742-6596/1204/1/012093)
20. N. T. A. P. Sari, N. R. Jayadi, N. P. Ramanda, N. Nurhasana, N. E. Angasa, *EduMatSains J. Pendidikan Matematika Dan Sains*. **8** (2024) 189 (https://doi.org/10.33541/edumatsains.v8i2.5574)
21. S. Zhu, Y. Song, X. Zhao, J. Shao, J. Zhang, B. Yang, *Nano Research* **8** (2015) 355 (https://doi.org/10.1007/s12274-014-0644-3)
22. T. Feng, Q. Zeng, S. Lu, X. Yan, J. Liu, S. Tao, M. Yang, B. Yang, *ACS Photonics* **5** (2017) 502 (https://doi.org/10.1021/acsphotonics.7b01010)
23. S. Qu, D. Zhou, D. Li, W. Ji, P. Jing, D. Han, L. Liu, H. Zeng, D. Shen, *Adv. Mat*. **28** (2016) 3516 (https://doi.org/10.1002/adma.201504891)
24. E. Yuniarti, A. Nurlaela, *J. Kimia Valensi*. **9** (2023) 253 (https://doi.org/10.15408/jkv.v9i2.34164)

25. L. D. Kasmiarno, A. Fikarda, R. K. Gunawan, I. Isnaeni, S. Supandi, N. S. Sambudi, *Waste Technol*. **9** (2021) 1 (https://ejournal.undip.ac.id/index.php/wastech/article/view/35922/pdf)
26. G. S. Das, J. P. Shim, A. Bhatnagar, K. M. Tripathi, T. Kim, *Sci. Rep*. **9** (2019) 15084 (https://doi.org/10.1038/s41598-019-49266-y)
27. K.J. Mintz, Y. Zhou, R. M. Leblanc, *Nanoscale* **11** (2019) 4634 (https://doi.org/10.1039/C8NR10059D)
28. Z. Wang, R. Changotra, M. Dasog, G. S. Selopal, J. Yang, Q. S. He, *Sustain. Mat. Technol*. **44** (2025) e01386 (https://doi.org/10.1016/j.susmat.2025.e01386)
29. C. Wang, Z. Ma, Z. Yao, P. Li, J. Zhang, W. Zhang, X. Zhao, J. Fan, *Colloids Surfaces, A* **711** (2025) 136416 (https://doi.org/10.1016/j.colsurfa.2025.136416)
30. J. Kong, Y. Wei, F. Zhou, L. Shi, S. Zhao, M. Wan, X. Zhang, *Molecules* **29** (2024) 2002 (https://doi.org/10.3390/molecules29092002)
31. Y. Wu, D. Qin, Z. Luo, S. Meng, G, Mo, X. Jiang, B. Deng, *ACS Sustain. Chem. Eng*. **10** (2022) 5195 (https://doi.org/10.1021/acssuschemeng.1c08676)
32. Y. Liu, W. Li, P. Wu, C. Ma, X. Wu, M. Xu, S. Luo, Z. Xu, S. Liu, *Sens. Actuators, B* **281** (2018) 34 (https://doi.org/10.1016/j.snb.2018.10.075)
33. S. D. Dsouza, M. Buerkle, P. Brunet, C. Maddi, D. B. Padmanaban, A. Morelli, A. F. Payam, P. Maguire, D. Mariotti, V. Svrcek, *Carbon* **183** (2021) 1 (https://doi.org/10.1016/j.carbon.2021.06.088)
34. E. O. Alegbe, T. O. Uthman, *Heliyon* **10** (2024) e33646 (https://doi.org/10.1016/j.heliyon.2024.e33646)
35. Y. Wang, Y. Huang, J. Lai, T. Chung, *Sep. Purif.. Technol.* **354** (2025) 128734 (https://doi.org/10.1016/j.seppur.2024.128734)
36. J. C. C. Ramirez, T. P. Tumolva, *Appl. Adhesion Sci.* **6** (2018) 1 (https://doi.org/10.1186/s40563-017-0102-z).